

Wireless Nanosensors and Systems (WiNS)

Gail McClure¹ and Vijay K. Varadan²
¹Vice President

¹Arkansas Science and Technology, Little Rock, AR

²Distinguished Professor of Electrical Engineering

²Distinguished Professor of Biomedical Engineering

²Director, WiNS Center

²University of Arkansas, Fayetteville, AR

ABSTRACT

Wireless Nanosensors and Systems research project has been investigating a systems approach to designing sensors systems. The effort is multifaceted and ranges from the design of low-cost sensors for various applications, such as biomedical or structural health monitoring, to the design of wireless interfaces and protocols with suitable networking and design of protocols to transmit sensor data from one place to another securely and to the design of appropriate applications themselves. The research team has been developing a system-engineering framework that forms the basis for collaborative activities across three campuses, University of Arkansas at Fayetteville, University of Arkansas at Little Rock and Arkansas State University, that captures the relationship between sensors, wireless interfaces, the network, the testbed that facilitates applications-level communications.

Keywords: Arkansas, science, technology, wireless, nanosensors, systems.

1. INTRODUCTION

The Arkansas ASSET Initiative has initiated a statewide infrastructure platform to support interdisciplinary research that we believe is enhancing Arkansas' competitiveness, creating added research and training opportunities, attracting top scholars, enabling Arkansas to form new links with national and international programs, and creating new economic opportunities for industry and entrepreneurship. To support the collaboration efforts between campuses, a student/faculty exchange program has been established. This program, managed by the Arkansas Science & Technology Authority (Authority) central office, provides stipends for travel and housing for extended stays on distant campuses. Since the three campuses are geographically separated, summer laboratory training and research collaboration opportunities are currently being organized for late May and June. Applications for the program are posted at the Authority website and are currently being reviewed by the executive management team.

Additionally, to strength research infrastructure on all campuses, ASSET Initiative has invested in expansion of access to eJournals. Electronic access to an expanded repertoire of full-text journals directly supports faculty research where it is most needed, which is most often research resources delivered in real time via the laboratory/office computer. This has been negotiated by the Arkansas Affiliation of the EPSCoR Information Support Group who have been awarded \$70,000 to expand the access of Arkansas universities to full text journal collections from publishers such as Springer, Blackwell, Taylor and Frances, etc. Although some universities have excellent resources, this is not universal for all campuses in all research disciplines. Additionally, the consolidated effort of group purchasing power has made many of these resources more affordable and expansion of resources more economically feasible.

The Wireless Nanosensors and Systems (WiNS) research effort is well on the way to forming a cohesive “virtual” center. This research collaborative has begun to form a strong consolidated and integrated research cooperative with both distance and on-site meetings of the expanded research teams. The research group held a retreat on April 12, 2008 to review campus progress and deliberate their strategic plans for the remainder of the grant cycle (see Figure 1 below).

| Yr 2 | Yr 3 | Yr 4 | Yr 5 | Yr 5-10 |
|---|---|--|---|--|
| Low voltage organic TFTs | Sensors integrated with printable RFID | System Engineering and Organic Electronic (OE) Systems: | System Engineering: POC monitoring devices Integration of OE systems with personal communication tools. | Total patient monitoring devices and POC testing devices for healthcare applications |
| OTFT sensors and Food and pathogen sensors | | | | |
| Wireless point of care (POC) sensors | System Engineering: Wireless POC testing and monitoring platforms | Real-time wireless POC monitoring devices for homecare | Data compression and secure network system implementation | Organic Polymer wireless systems |
| POC testing devices; Neural substratums and animal models | | | | |
| Wireless data security Modeling Energy scavenging networks High performance computing | Compatible power sources for the above | Technology transfer | Technology transfer | Nanoelectronic and Neuroelectronic chips |
| Nanoantennas, multiscale continuum models for ZnO /CNT materials for sensing | | | | |
| Solar Power generation Sustainable power sources | 2 day summer camp | Technology transfer | New curriculum for Nanotechnology/ neuroelectronic devices | |
| Summer camps and workshops Site visits collaborations | | | | |
| Proposal submissions Faculty supports | | | | |

Figure 1. Strategic plans for Wireless Nano-Bio-Info Sensor & Systems Research

2. FINDINGS OF WIRELESS NANOSENSORS AND SYSTEMS RESEARCH

Goals of the WiNS Center were (i) to develop and optimize nanomaterials and nanostructures for sensing applications and power generation; (ii) to develop nanotechnology platforms for the neuron growth along with infrastructure development; and (iii) develop organic thin film transistors and wireless protocols for the integrations of these sensors for system engineering. Following sections present the research findings to achieve the above goals.

2.1 Nanomaterials and Nanostructures

2.1.1. Carbon Nanotube Synthesis and Characterization: Experiments were conducted using microwave chemical vapor deposition system to synthesize multiwall carbon nanotubes (MWCNTs). The system works at a frequency of 2.45 Hz and in a power range of 0 to 3000 W. The catalyst used here is Iron-magnesium cobalt mixture. The reaction gases- Ar and acetylene were introduced at one end and the exhaust gases were let out from the other end. The mass flow controllers were used to control the flow of the gas and time span with the catalyst. The catalyst, about 50 mg was dispersed on the silicon carbide substrate to form a thin layer with approximate thickness of 1.5 mm on the substrate. After the substrate was loaded in the cavity, argon gas

purged at 100 sccm into the cavity and microwave power was switched on and the substrate is heated to about 700°C. The layer of the catalyst on the silicon carbide should be as thin as possible and should be laid out evenly. It is observed that thicker layer deposited would yield more of amorphous carbon than MWCNTs. Varying the process parameters, such as flow rates of gases and time span with catalyst have resulted in different diameters and lengths of the obtained MWCNTs. It was also observed that the yield of the carbon nanotubes (CNTs) decreased when sufficient gases and flow rate was lower than the required.

2.1.2. Vertically Aligned Multiwalled Nanotubes on Microelectrode Arrays.

The primary aim is to grow vertically aligned CNTs on microelectrode arrays. All fabrications steps were conducted at the UAF clean room facilities. The microelectrode arrays are created on a 5" single side polished <111> wafer. The arrays are patterned using photolithography and the electrode lines and the catalyst layers are defined using an electron beam evaporator for thin film deposition. The patterned wafers are then prepared for metal layer deposition in an e-beam evaporator. The MEA are fabricated using thin films of gold. In order to promote adhesion of the gold thin film a 50Å thick film of titanium is first deposited followed by a 1000Å thick layer of gold. The adhesive layer thickness was varied to determine superior binding of the gold thin film to the surface. In order to synthesize CNTs on the MEA a catalyst layer is deposited using an e-beam evaporator. A 50Å thick layer of chromium is deposited to improved adhesion of the iron/nickel layer to the gold MEA. The catalyst layer thickness was varied from 10-50nm. Initial experiments utilized Ti as the adhesive layer between Au and Fe/Ni thin films. The wafers are then placed in an acetone bath for stripping the photo resist and later diced. The diced wafers are then placed in a microwave CVD chamber and heated to a temperature of 700°C in the presence of argon as a purging gas at a flow rate of 100sccm. Acetylene gas is introduced at a flow rate of 30sccm for 30mins followed by cooling in an argon atmosphere. The samples are then examined using a JEOL scanning electron microscope. Figure 2 presents the SEM pictures of aligned CNTs on microelectrode array.

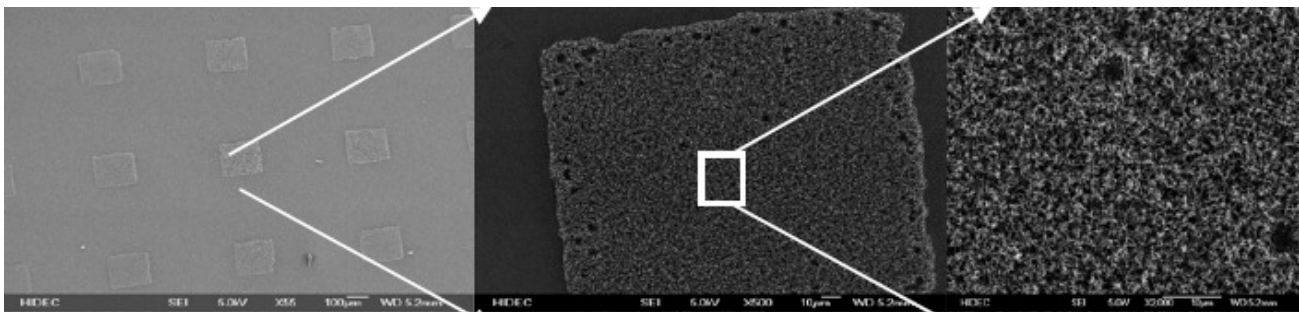


Figure 2 presents the SEM pictures of aligned CNTs on microelectrode array.

Despite good CNT formation of the Ti/Ni, this combination was abandoned due to the toxic effects of Ni. The optimum thin film layers were determined to be Ti-Au-Cr-Fe for use in MEA/CNT assisted system for neural growth control. Also the CNTs were observed to be only quasi-aligned. After elimination of catalyst layer thickness as a possible cause, reaction times and mass flow of acetylene gas were varied. Reduction agents (H₂, forming gas and ammonia) were utilized during the reaction process, in combination with Ar purging gas, to account for oxidation of the iron thin films. The CNTs were functionalized by keeping it in potassium permanganate solution which acts as an oxidant in the presence of acetic acid and a phase transfer agent. The functionalization process demonstrates satisfactory surface adhesion of the CNTs to the substrate for neurite growth.

2.1.3. Magnetic Nanotube synthesis:

The magnetic nanotubes were fabricated using AAO template method. The AAO templates are first soaked in an ethanol solution for 30 mins. A 25% solution of $\text{Fe}(\text{NO}_3)_3 \cdot 9\text{H}_2\text{O}$ and ethanol is forced through the AAO template with 200nm pores and a filter. The templates are then dried at 60°C for 45 mins. This is followed by thermal decomposition in air at 250°C followed by thermal annealing at 600°C. After SEM observations, magnetic properties of the nanotubes were measured using the Vibrating Sample Magnetometer. The hematite nanotubes were found to be weakly magnetic. In order to improve the magnetic properties the templates are reduced in a hydrogen atmosphere at 500-700°C for 10-15hrs.

2.1.4. Fabrication of CNT electrodes for Glucose sensor:

Carbon paste-based and carbon nanotube based electrodes were fabricated to for glucose sensing application. The carbon paste for the sensing electrode was prepared by mixing carbon materials (graphite, glassy carbon, carbon nanotubes and platinum-decorated nanotubes), mineral oil, ferrocene-based mediator, and glucose oxidase in a proper ratio at room temperature. Then the carbon paste was pressed into a Teflon electrode housing with a platinum wiring out and kept at 4 °C before testing. The electrochemical characterization of the electrode was conducted on a three-electrode cell in which the working electrode was immersed into a phosphate buffer solution (PBS) with a platinum counter electrode and a Ag/AgCl (3 M KCl) reference electrode. All electrochemical measurements were performed on a Solartron 1287 electrochemical station.

2.1.5. Nanotubes for glucose sensing

For glucose-sensing testing, a potential of +0.65 V (vs the reference electrode) was applied on the working electrode and let the background current decay to a stabilized value. Then equal amount of 5 μmol of glucose were successively added into the phosphate buffer solution with a mild magnetic stirring, and the responding current signal was recorded. In our experiments, the responding current should rise up and saturate to a higher current value with an addition of 5 μmol glucose. Compared with the background current, the saturated current signal is expected to be linearly proportional to the glucose concentration. A good sensing linearity can be seen for glucose concentration up to 28 mM, which implies a wide glucose detecting range for the Pt/CNT paste-based electrodes. Additionally, the slope of the curve could be defined as the current value change for an increment of 1 mM glucose concentration.

2.2: Nanotechnology Platforms for Neurite Growth

2.2.1. Neurite growth on Magnetic Nanotubes

The synthesized magnetic nanotubes have been used in the study of neuron culture, which is conducted in collaboration with Arkansas State University. It is found that magnetic nanotubes are attached to the surface of neurite, confirming that magnetic nanotubes are non-toxic to neurons. As shown in Figure 3, neurites navigate across magnetic nanotubes laid on the substrate. Meanwhile, many magnetic nanotubes locate on the surface of neurites implying a non-repulsion, non-toxic interaction between neurites and nanotubes. It is also experimentally confirmed that the tubular structure of magnetic nanotubes can be used for the delivery of nerve growth factor (NGF) which is required for the differentiation and growth of PC 12 cells, and the magnetic fields produced by magnetic nanotubes appears to be favorable for the growth of neurites. The crystalline structure and magnetic properties of the magnetic nanotubes are characterized.

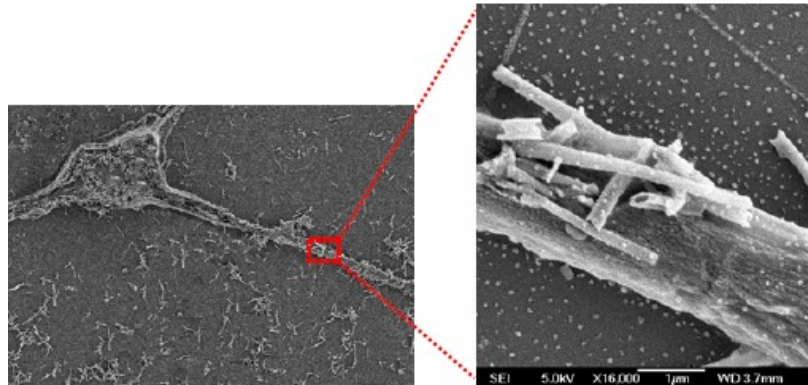


Figure 3. SEM micrographs of magnetic nanotubes attached to the surface of a neurite.

2.2.2. Design of Nanowire Electrodes

Nanowire integrated Microelectrode arrays: Nanowire electrode arrays based on Nanowire Electrode Ensembles (NEE) of gold and conducting polymer (polypyrrole) were designed and fabricated. Vertically aligned nanowires were fabricated using hybrid membrane attachment and electrochemical deposition processes on a glass or a polyimide substrate. Sodium aurosulfite, $\text{Na}_3\text{Au}(\text{SO}_3)_2$ solution was used to grow gold nanowires, while a solution of pyrrole and sodium dodecylbenzenesulfonate (NaDBS) was used for polypyrrole nanowires. After growth of nanowires, the photoresist and membrane were removed using IPA and dichloromethane solution. Electrical feed lines were then defined from the nanowire platform to the electrical probe pads with the electropolymerization was applied after fabrication of Au microelectrodes allows us to easily modify the gold electrodes to create gold/polypyrrole structures.

For nanoelectrodes, their electrochemical impedance was measured that an Au nanoelectrode with $1600 \mu\text{m}^2$ geometric area has impedance values from 2.8 k Ω to 1.02 M Ω in frequency range from 0.1 Hz to 100 kHz, which is significant reduction of impedance was observed over 10 times on overall frequency range, as compared to planar electrodes. Cell growth test results: In order to check biocompatibility of nanoelectrodes, neural cell growth test was performed at Arkansas State University (Srivatsan). Electrodes were coated with poly-D-lysine and PC 12 cells were cultured with nerve growth factor. After cell growth, SEM observations showed that the cell adhesion and differentiation appeared to be different between the nanowire electrode surface and the planar electrode surface. In comparison to the planar electrodes, the nanowire electrodes appeared to provide preferential growth sites, probably due to their unique structure.

2.2.3. Carbon/magnetic nanotube functionalization and Neuron culture:

Figure 6 shows scanning electron microscope micrograph revealing an obvious neurite outgrowth from the cultured neurons plated on a functionalized carbon nanotube mat. It is easy to differentiate the neurites from the carbon nanotube background due to their bigger diameter. Besides single neurite, bundles of neurite extended from the same neuron and neurite branching were also observed. This multiple neurites growth may suggest that the potential for growth has increased in neurons when cultured on functionalized carbon nanotube mat. Neurons cultured on unfunctionalized carbon nanotube mat also showed a few growth-cone formation and neurite extension. However, much shorter neurites were observed.

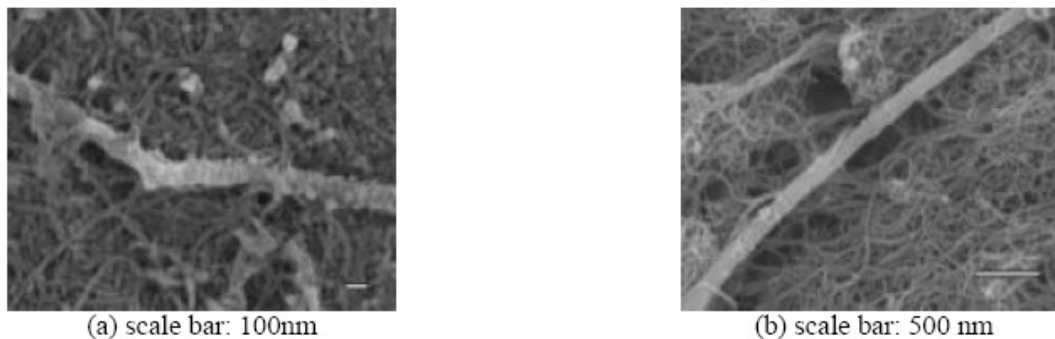


Figure 4. Neurites grown on the carbon nanotube mats as the substrates. (a) on functionalized carbon nanotubes, (b) on unfunctionalized carbon nanotubes.

Figure 4(a) and 6(b) present high resolution SEM micrographs showing the neurite interaction with unfunctionalized and functionalized carbon nanotube mats, respectively. As shown in Figure 4(a), a neurite was grown over unfunctionalized carbon nanotubes with a weak interaction between them. On the contrary, neurites intertwined with the functionalized carbon nanotubes indicating a strong interaction between them, as can be seen from Figure 4(b). This close contact in nanoscale could have enhanced the growth of long neurites in culture. It was reported that the surface charge of carbon nanotubes can modulate the neurite growth and branching. Thus we proposed that the functional groups could act as anchoring seeds for neurite growth across the functionalized carbon nanotube mat.

Compared with unfunctionalized carbon nanotubes, the functional groups attached to nanotubes may assist better the extension of neurites. It was found that functionalized carbon nanotube provide a permissive substratum for neurite growth. It is believed that the strong interaction in nano scale between neuron/neurite and carbon nanotubes enhances the neurite outgrowth.

2.2.4 PC 12 cells cultured in presence of magnetic nanotubes

We also demonstrated the effect of nerve growth factor-incorporated magnetic nanotubes for both PC 12 cell differentiation into neurons and neurite growth. PC 12 cells were chosen for this study because these cells require NGF to differentiate into neurons and any sign of differentiation will be indicative of the availability of NGF from the nanotubes to the PC 12 cells. For SEM observation, to avoid cell morphology deformation during the sample drying process, the critical point drying method was applied. SEM micrograph Figure 5(a) shows an appreciable neurite outgrowth. Major components of a growing neuron including soma, neurites, and growth cone can be discerned, suggesting that the nanotube bound NGF was available to the PC 12 cells to induce neuronal differentiation. The enlarged SEM image (Figure 5(a)) shows the growth cone area, located on the tip of the axon, where slender extensions, the filopodia were formed towards the nearby magnetic nanotubes. High-resolution SEM micrographs reveal more details about the growing processes, hematite nanotubes, and their interactions. Figure 5(b) shows that the filopodium made a contact with the nanotube.

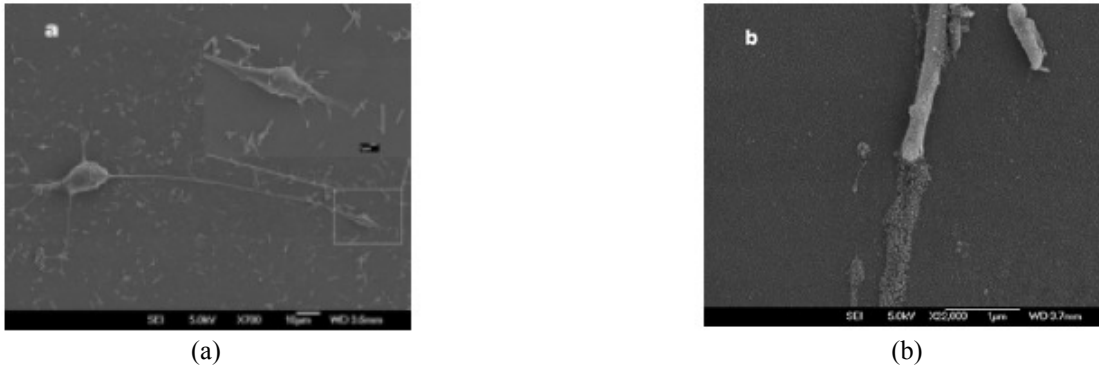


Figure 5. PC 12 cell culture with NGF-incorporated magnetic nanotubes: (a) SEM micrograph of a typical PC 12 cell with cell body and neurites (the inset is a magnified image of the growth cone area); (b) high-resolution SEM micrograph of a NGF-incorporated hematite nanotube and its interaction with a filopodium.

2.2.5. Nanowire electrodes and Neuron compatibility: In a second set of experiments, ASU team cultured neurons on nano electrodes to provide feedback on improving the design of the electrodes with vertically aligned nanowires fabricated at UAF. The fabrication process of nanowire electrodes has been optimized to yield highly efficient sensing and stimulation of neural signal. Figure 6 shows the neurons (in green) are grown on gold nanoelectrode wires which can be used to stimulate and record electrical activity of these neurons. Beta tubulin in neurons were stained immunocytochemically using appropriate antibodies. The results show that the nanowire electrodes were neuron compatible and neurites grew from neurons cultured on nano electrodes coated with polylysine. They appeared to show a preference to grow around the vertically aligned nano wires. These results also showed that the central cylinder needed to be bonded using a better, permanent and bio compatible adhesive. This feedback is helping to modify the design of the electrodes to improve performance. We are currently repeating these experiments on the nano electrode wires made with an improved design.

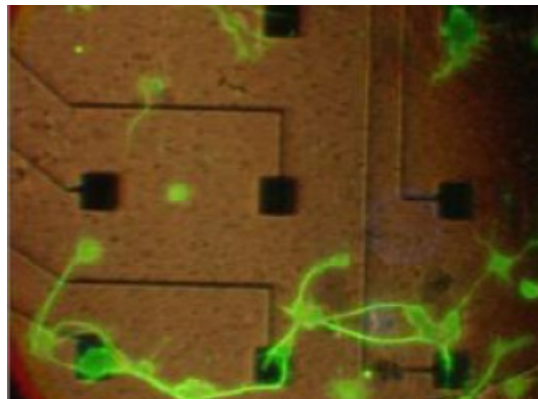


Figure 6. Fluorescent microscope images of neurons cultured on nanowire electrodes

2.2.6. Nanomaterials to enhance the power generation:

Experiment: Ten different samples were synthesized to characterize the ZnO nanostructures. The sample was placed face up in a glass beaker which was then filled with 20ml of 10 ppm Methylene Blue (MB) solution. This setup was then placed under a UV lamp for 1 hour. The absorbance of MB solution in the beaker was then measured using a UV/Vis Spectrophotometer. By taking Beer-Lambert law into account the Figure 7 was

plotted after measuring the respective absorbance values of 2ppm, 4ppm, 6ppm, 8ppm and 10ppm MB solutions.

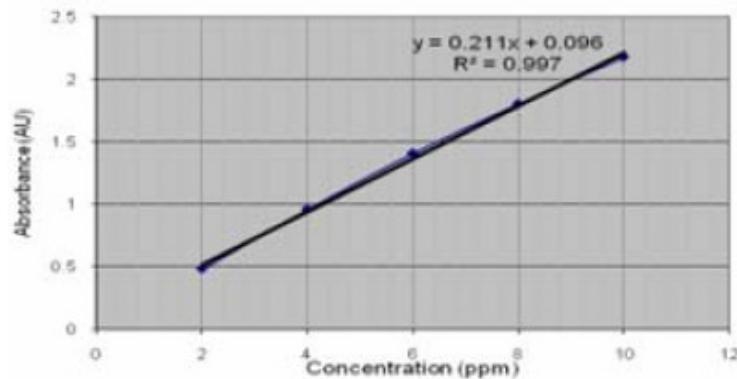


Figure 7. Absorbance vs concentration of the sample synthesized for the solar cell using ZnO nanostructures.

After 1 hour of photocatalysis, the MB solution decomposed from 10ppm in each case to the values shown above. From the above results, one can clearly observe that the samples with the secondary structures decompose the MB solution better. However, one must note that sample 17 weighed 0.7068 gms and sample 15 weighed 0.5506 gms. Photocatalysis with close sample weights must be done before reaching any conclusions. If a lighter secondary sample decomposes better than a heavier primary sample, that result would be conclusive.

2.3 Organic Electronics and Wireless Systems Integration:

2.3.1 Organic Electronics Thin Film Transistors:

Pentacene TFTs based on a bottom contact configuration have been fabricated on a highly doped n type silicon wafer ($<0.005 \Omega\text{cm}; <100>$ orientation) as shown in Fig 8 (a. upper). The highly doped silicon and 200 nm of thermal SiO₂ serves as the gate electrode and dielectric, respectively. A 120 nm thick layer of palladium was first e-beam evaporated, and patterned to define the source/drain contacts. Then, pentacene obtained from Aldrich (97% purity) without further purification was deposited onto the gate oxide by thermal evaporation following the treatment of the oxide surface with octadecyltrichlorosilane (OTS). The nominal channel length and width of TFTs, in which the pentacene active layer is exposed to air without any encapsulation, is 60 and 300 μm , respectively.

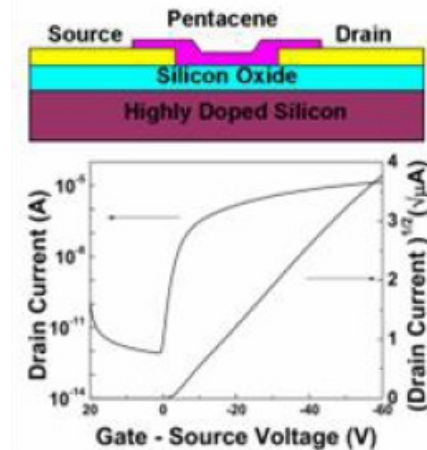


Figure 8. (a) Schematic cross-sectional view of a bottom-contact pentacene TFT without encapsulation. (b) transfer characteristic, measured at RT, of such a bottom-contact pentacene TFT with a channel length and width of 60 and 300 μm , respectively.

From the transfer curve of the bottom-contact pentacene TFTs measured at room temperature [See Fig. 8 (b, lower)], we extract a saturation mobility 0.086 cm^2/Vs , and an on/off current ratio $> \sim 10^7$ at a drain-source voltage (VD) of -60V. For annealing tests, the TFTs were kept for 1hour at a given annealing temperature, and cooled down to RT (30 oC) to measure the transfer curves. This procedure was repeated with the same device for different annealing temperatures of 50, 70, 100, 120, and 160 oC. The dependences of resulting mobilities on annealing temperatures for three other TFT samples that were processed together on the same substrate are well shown in Fig. 12, where the carrier mobilities are normalized with respect to their highest mobility value ($N\mu = \mu/\mu_{\text{max}}$). The mobility values of all the samples tend to increase with increasing annealing temperature, and reach to peak values ($N\mu = 1$) at 70 oC even though the highest values range from 0.092 to 0.12 cm^2/Vs .

2.3.2. Wireless Sensor Platforms:

A wireless system platform which has plug-and-play capability is developed at UAF as shown in figure 9. This wireless system will be utilized for the future sensor integration. The analog inputs from the sensors are first processed through a signal conditioning unit for noise filtering, level shifting and other functions depending on the type of sensor output. The ADC then converts the analog inputs to digital data with a 12-bit resolution. An external voltage reference is used in the conversion process. This ADC can either be internal to the microcontroller or an external one communicating with the microcontroller through the SPI interface. This data is then packetized in the proper format for multi-channel data transmission and sent via the UART interface to the wireless module. This wireless module can be Bluetooth, Zigbee or any other module which is capable of providing sufficient bandwidth for error-free transmission of the sensor data. Power to the system is provided by a Li-Polymer rechargeable battery pack (3.7V, 1700 mAh). A DC/DC converter based step-up circuit is used to convert this voltage to +5V and +3.3V supply rails required by different parts of the system.

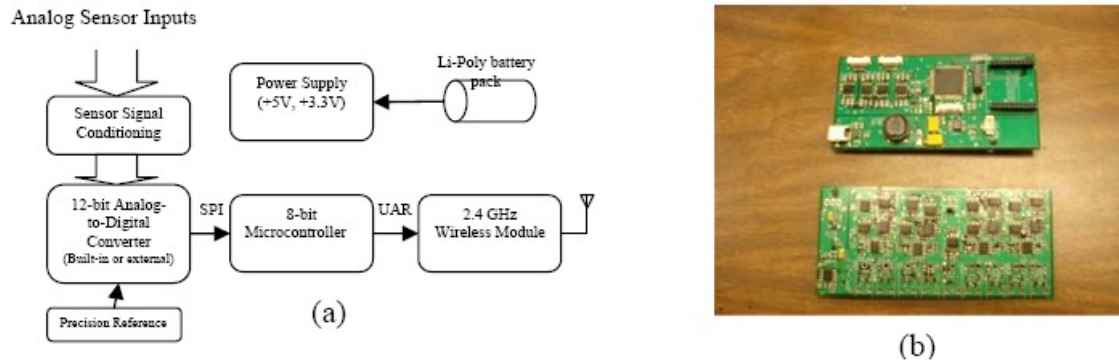


Figure 9. (a) Schematic diagram of the wireless platform developed for the system integration; (b) photograph of the wireless boards developed at UAF.

2.3.3. Systems Engineering: Architecture and Integration:

The objective of the systems engineering research at UALR for the wireless sensors network system is to fill the need by applying systems engineering principles in the design of the general architecture and in the integration of its components. The system architecture process must assure the accomplishment of both the primary system functions that have immediate value, as well as the system secondary functions that have life-cycle value. To obtain a measure of the overall system architecture effectiveness, the system architecture characteristics need to be translated in measures of system performance and efficiency. A systems engineering test-bed to be developed at UALR with participation from the Computer Science and Systems Engineering Departments will complement the theoretical findings for the needed system architecture and integration characteristics.

The research has so far specified the general system architecture and identified the needed secondary functions (responsiveness, availability, modularity, scalability, affordability) and provided their definitions in the context of the wireless sensors network system architecture. Using the proposed systems engineering integration testbed, the system architecture characteristics identified above will be evaluated and recommendations will be made in terms of which of those secondary functions are more desirable for certain types of applications. As an important step in the system design process, building the system architecture helps in moving forward the design process. To stand the tests of time and feasibility, the architecture of large-scale systems, such as wireless sensor networks, need to address the characteristics identified above. Future work will focus on, in collaboration with researchers across the three campuses, defining both quantitative and qualitative performance measures for these characteristics such that they can be easily included in the design process and monitored during system operation.

2.3.4 Microstrip Antennas Based on Carbon Nanotubes

Most of the antenna studies based on CNT were intended to understand the physics of current flow in the nanotubes and hence evaluate the impedance and the field distributions around the nanotubes. The propagation of the surface waves in CN's has to be considered. The phase velocities and the slow-wave coefficients of surface waves will be explored for a wide frequency range, from the microwave to the ultraviolet regimes. Also, attenuation and retardation in metallic and semiconductor CN's will be considered. It is obvious the carbon nanotubes are in the nano scale "length and diameter", which makes it is very difficult to operate as a traditional antenna in the microwave range "several centimeters". One of the approaches in this project is to connect between CNT's using the functional group. The antenna element includes carbon nanotubes structure constituting a network scheme having plural carbon nanotubes electrically connected to each other. The process

for producing the microwave antenna includes applying plural carbon nanotubes each having a functional group to a surface of the substrate and cross linking the functional groups a chemical bond to form a cross linked part.

2.3.5 User-Based Channel Assignment Algorithm in a Load-Balanced IEEE 802.11 WLAN

A new load balancing algorithm is developed based on power management of Access Points (APs) to reduce congestion at hot spots in Wireless Local Area Networks (WLANs) and to assign channels to APs. The algorithm first finds the Most Congested Access Point (MCAP), then decreases its transmitted power in discrete steps, and the process continues until the users' assignment which leads to a high balance index is reached. A new mathematical formulation is then applied to assign channels to the APs such that the Signal-to-Interference Ratio (SIR) is maximized at the users' level. Results show that the algorithm is capable of reducing the overall congestion at hot spots in a WLAN and increases the SIR by more than 100% for cases involving relatively large WLANs, which in turn significantly improves the network throughput.

2.3.6 Multiscale Continuum Analysis of Wave Propagation in Nano Sensors with Complex Nanostructures

Understanding and describing the high-frequency dynamic properties of ultra-thin films with complex nanostructures are fundamental concerns and challenging problems in designing and predicting performance of micro- or nano-sensors. The goal of the research is to develop a multiscale continuum theoretical and computational basis for the analysis of THz wave propagation in the ultra-thin films. Emphasis is on predicting nanostructure effects. Specifically, it consists of the following major parts: (1) developing an atomistic-based multiscale microstructure continuum theory that represents dynamics behaviour of ultra-thin films to capture the nanostructure effects, which is computationally more efficient than molecular simulation without introducing any additional unknown material constants compared with the existing high-order continuum theories; (2) extending the proposed theory to consider nanostructure effects on the multiple fields, including electro-mechanical coupling dynamic behaviour, phase transformation, and thermal properties; (3) performing the developed multiscale microstructure theory to understand, predict, and characterize the nanostructures of the ultra-thin films in a nondestructive way by using surface acoustic linear and nonlinear wave propagation and new physical phenomena by using THz surface acoustic waves.

2.3.7 Energy-aware routing in Wireless Sensor Networks

The UALR team has investigated a Consumed-Energy-Type-Aware Routing (CETAR) that can extend the lifetime of the WSNs. CETAR uses statistics of the energy consumed for each type of node activities including sensing, data processing, data transmission as a source node, and data reception/transmission as a routing node for routing decision. In particular, CETAR selects a node with high residual energy which seldom plays a role of source node as a routing node. Idea is to maintain the energy of active source nodes to prolong the functionality of the WSNs. Biased Consumed Energy (BCE) derives a bias factor for a node that frequently plays a role of routing node and a node that frequently plays a role of source node. Aggressively-and-Adaptively BCE (AABCE) further extends BCE by dynamically adapting the extent of the bias factor among consumed-energy types as the amount of consumed energy at each node changes. With its adaptability to hierarchical network, the significance of CETAR to extend the lifetime of WSNs is clear.

2.3.8 Wireless Ad-hoc Network Test-bed

A Wireless ad-hoc network test-bed has been designed and its implementation is progressing. This test-bed consist of Crossbow motes, localization devices (bacons and a listener), software development kit (SDK), and handheld communication system (PDAs/cell phones and 802.11 access point). The SDK will be used to implement and integrate proposed protocols to off-the-shelf systems. A set of motes and base station connected via different frequency domains will be employed to characterize the effect of proposed protocols in different data communication environments. The localization device will be used to test effectiveness of location-aware protocols such as location-aware routing and cluster formation. The handheld communication system will be used to test new ideas to resolve reliability and security issues in handheld-based systems and applications. This test-bed will allow researchers to evaluate their ideas in the real system. The development of a prototype sensor network in healthcare environment is currently progressing. This system will track patterns of hand-washing and other activities of health professionals so that a health care facility may be able to mount appropriate intervention procedures that facilitate the adoption of healthy, hygienic practices that will significantly reduce incidence of preventable infection.

2.3. 9. Secure Communication

UALR research team conducted investigations for intrusion detection and developed protocols for secure communications. Identifying and addressing code injection vulnerabilities in a dynamic manner (often with as little as 500 low-level system commands) is critical to enhance an application's reliability and its adoption in the the real world, especially for systems such as WSNs which are highly memory restricted. This investigation as the potential to impact various locations to support and sustain such a development process.

3. SUMMARY

Wireless Nanosensors and Systems research project have been investigating a systems approach to designing sensors systems. The effort is multifaceted and ranges from the design of low-cost sensors for various applications, such as biomedical or structural health monitoring, to the design of wireless interfaces and protocols with suitable networking and design of protocols to transmit sensor data from one place to another securely and to the design of appropriate applications themselves. They have developed a systems engineering framework that forms the basis for collaborative activities across campuses that captures the relationship between sensors, wireless interfaces, the network, the middleware that facilitates applications-level communications and the applications. After the successful development of the individual components as outlined above, the system integration will start early Yr2 as shown in the table. The sensors developed at UAF will be integrated to the wireless systems which have necessary security and privacy protocols, developed by the UALR team. The models developed for the optimization of the nanosensors will be helpful for designing and integrating it into the wireless test-beds.

ACKNOWLEDGMENTS

WiNS Center is supported by the United States National Science Foundation (NSF) under the project EPS-0701890 and the CFDA# 47.080. The research work performed by the groups led by Vijay Varadan, Seshadri Mohan, Srini Ramaswamy and Malathi Srivatsan is greatly acknowledged